振動円柱まわりの粒子流の時間平均場と局所衝突効率

Time-averaged field and the flux distribution of particle flow around an oscillating circular cylinder

坪井一洋, 茨城大・工, 〒316-8511 日立市中成沢町４－１２－１, E-mail:tsuboi@dse.ibaraki.ac.jp
木村茂雄, 神奈川工大, 〒243-0292 厚木市下荻野１０３０, E-mail: skimura@mserver.me.kanagawa-it.ac.jp
TSUBOI Kazuhiro, Ibaraki Univ., Naka-narusawa 4-12-1, Hitachi, 316-8511, JAPAN
KIMURA Shigeo, Kanagawa Inst. of Tech., 1030 Shimo-ogino, Atsugi, 243-0292, JAPAN

We perform numerical simulation of two-dimensional particle flow around a circular cylinder at rest and in oscillation based on 2-fluids model of dusty gas and investigate the effect of cylinder oscillation to the mass flux of particle flow (namely local impingement efficiency). Incompressible potential flow is employed as the main flow field for the simplicity. Based on the computational results, the distribution of mass flux along the cylinder surface and the total amount of particles impacting the cylinder are obtained as a function of the induced frequency in pitching and/or heaving oscillation. We also investigate the time-averaged particle flow field and attempt to clarify the feature of the flow field around an oscillating circular cylinder.

1. INTRODUCTION

Flows including a huge number of small particles are observed frequently in natural circumstance or in industrial fields.(1) As some examples of this composite flow, we can take flow of dusty gas and droplet flow: in the former example solid particles suspend in main flow of gas or liquid while liquid particles in gas for the latter.

The equation of flows including particles was originally derived by Saffman in order to investigate the flow stability of dusty gas.(2) Researches on this equation have achieved and some theoretical aspects have been clarified.(3)-(4) Recently, the authors employ this equation to icing problem as a model of super-cooled atmosphere.(5) Based on this approach, accumulated ice on a body surface is simulated numerically and some kind of accreted ice is reproduced successfully.

One of the most important problems in dynamics of flows including particles is to understand how particles impinge on a body surface. In fact, there seems to be two typical questions on this problem: criteria of particle impingement and the profile along a body surface.

In the case of placing a body in uniform flow of particles such as dusty gas, there exists a finite limitation of parameter known as Stokes number. When the Stokes number is smaller than the threshold, no particle reaches at the body surface.(6) To clarify the threshold in several flow conditions is, therefore, in vital importance.

On the other hand, when particles can reach at the body surface, the distribution of particle impingement, which is called the local impingement efficiency, becomes important knowledge. In fact, the local impingement efficiency plays an essential role in simulating shapes of accreted ice in icing problem.

An experimental result is presented in Fig. 1 to show the effect of the local impingement efficiency. In this experiment, a circular cylinder is placed in uniform flow of super-cooled atmosphere and the growth of accreted ice on the cylinder is observed. In particular, the cylinder is given two kinds of oscillating motion, *i.e.* pitching and heaving. From this experiment, we obtain the following results.(7)

(1) The effect of oscillating motion of body to ice accretion process appears at the beginning of the formation.
(2) Pitching motion seems to affect more greatly than heaving motion.

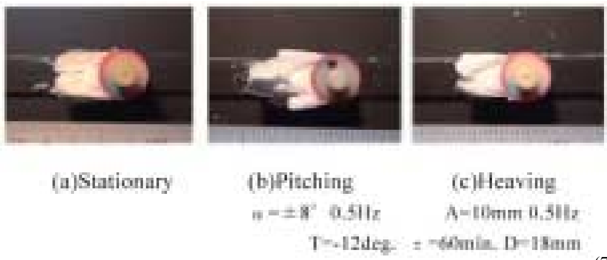

Fig. 1. The effect of oscillation to the accreted ice.(7)

In the present study, particle flow around a circular cylinder in oscillation is computed based on the Saffman's equation of dusty gas. Then, incompressible potential flow is employed in main flow for the simplification. Time-averaged values of the local impingement efficiency along the cylinder surface and the total collision efficiency are obtained from the computed flow fields. Discussion on the experimental result is also presented based on the computed results. This research will give some useful information to the investigation of ice accretion on a body such as an electric power line. (8)

2. MATHEMATICAL MODEL

We consider the basic equation of dusty gas, which was derived by Saffman in order to investigate the flow stability.(2) It is true indeed that his equation was used to describe flows including a huge number of solid particles in gas or liquid. However, it is obvious that the equation is applicable to another class of composite flows as long as the effect of deformation of each particle is negligible. We actually take such an example as droplet flows, in which water droplets flow with main airflow such as super-cooled fog.

When Stokes drag formula is employed for the simplicity, the equations of particle phase (*i.e.* mass and momentum equations of particles) written in non-dimensional form are easily derived as follows [9],

$$\frac{\partial \eta}{\partial t}+\frac{\partial}{\partial x_j}(v_j\eta)=0\ , \qquad (1)$$

$$\frac{D}{Dt}(v_i)+\frac{1}{\tau}(v_i-u_i)=0\ , \qquad (2)$$

where v_i and u_i mean the velocity field of particles and main flow, respectively. The quantity η indicates the mass density of particles and the effect of mass change is neglected here for the simplicity. It should be noted that the particle density does not affect the velocity field of particle flow and that this fact is not subject to the Stokes law.

The parameter τ included in eq.(2) is a non-dimensional form of a coefficient of the particle resistance term defined as

$$\tau^{-1}\equiv 3\pi\mu\frac{\bar{d}}{\bar{m}}\frac{L}{U}, \qquad (3)$$

which means the non-dimensional relaxation time of particle motion, namely the Stokes number.

On the other hand, as the basic equations of main flow we can adopt, for example, the incompressible Navier-Stokes equations,

$$\frac{\partial u_j}{\partial x_j}=0\ , \qquad (4)$$

$$\frac{\partial u_i}{\partial t}+u_j\frac{\partial u_i}{\partial x_j}=-\frac{\partial p}{\partial x_i}+\frac{1}{R}\Delta u_i+\frac{\eta}{\tau}(v_i-u_i)\ . \qquad (5)$$

where R is Reynolds number.

The reaction from particle flow appears in the third term of right hand side in eq.(5) and this effect is proportional to the particle density. This term, however, becomes small within the present model, in which the effect of collision between particles is completely neglected.

Here, we consider flow of super-cooled fog as an example. Amount of water included in air of unit volume is called Liquid Water Content (L.W.C.) and the value of L.W.C. in natural wind is at most 1 g/m^3. The ratio to air density is, then, in order of 10^{-3}. This estimation leads to the conclusion that main flow is not affected by the particle flow and it is possible to consider that the behaviour of main flow is determined by itself. The solution of Navier-Stokes equations (4) and (5), therefore, is not necessary as long as the viscous effect can be neglected.

Based on the above consideration, we can employ potential flow around a circular cylinder with the circulation in arbitrary motion in uniform flow as a model of main flow.[10] In this model, circulation gives approximately the effect of pitching motion and translation of heaving cylinder is reproduced as one typical option of arbitrary motion.

In the heaving motion of the cylinder perpendicular to the uniform flow, the induced frequency (k_h) and non-dimensional amplitude of heaving motion (γ_h) are defined as follows,

$$k_h\equiv\frac{A\omega}{U},\quad \gamma_h\equiv\frac{A}{2a}. \qquad (6)$$

where A and a indicate the amplitude and the radius of the circular cylinder, respectively.

On the other hand, the induced frequency (k_p) and the effective angle (γ_p) in the case of pitching oscillation are given as

$$k_p\equiv\frac{a\Theta\omega}{U},\quad \gamma_p\equiv\frac{\Theta}{2}\, , \qquad (7)$$

where Θ indicates the maximum angle of pitching amplitude.

Finally, we summarize the computational technique used in the present simulation. On the treatment of the basic equations, we can take de-coupling of eq. (1) from eq.(2) since the particle density η does not appear in eq.(2). This means the particle density is obtained passively from the velocity field of particles.

Equations (1) and (2) are discretized on body-fitted coordinates system by using finite difference method. In particular, fine distribution of grid points near the cylinder surface is used since it is known that thin layer of particle free along the surface forms when τ is small.[3] On the discretization of convective terms in eqs. (1) and (2), third order upwind difference scheme is employed, in which the fourth order numerical viscosity is added to the original term.[11] Moving grid technique[12] is also introduced in order to simulate heaving and pitching motion of a circular cylinder. Then, convective terms in eq.(1) and (2) are rewritten respectively

$$\frac{\partial(\eta v_j)}{\partial x_j}\rightarrow\frac{\partial(\eta v_j)}{\partial x_j}-w_j\frac{\partial\eta}{\partial x_j}+\frac{1}{4}|v_j-w_j|\frac{\partial^4\eta}{\partial x_j{}^4},$$

$$v_j\frac{\partial v_i}{\partial x_j}\rightarrow(v_j-w_j)\frac{\partial v_i}{\partial x_j}+\frac{1}{4}|v_j-w_j|\frac{\partial^4 v_i}{\partial x_j{}^4},$$

where w_j means the velocity of each grid point.

In eqs.(1) and (2), absorbed condition is employed on the body surface in upstream side, in which particle flow can penetrate the surface and then it is removed from the flow field. On the other hand, no-penetration condition is imposed on the surface in downstream side, because the absorbed condition in this side could cause source

3. COMPUTATIONAL RESULTS

In this section, we present some computational results. Computations of a stationary circular cylinder have performed on grid system of 200 by 200 points with O-type topology while those of oscillating cylinder have done on 100 by 70 grid system.

3.1 Stationary Circular Cylinder

Some results of a stationary circular cylinder are shown in order to compare them with results of oscillating cases. The solutions of all cases under consideration reach at steady state rapidly because of steadiness of main flow.

The velocity and density fields of particle flow in steady state are depicted in Fig. 2 to four different values of τ in order to overlook the behaviour of particle flow. From this figure, we can survey the variation of particle flow according to the parameter τ.

When τ is infinite, no interaction between main flow and particle occurs and particle flow is independent of main flow, in which velocity and density of particle is uniform except the wake region (see (a)). Decreasing the value of τ, particles accumulate in the front region of the cylinder since the motion of particle decelerates near the stagnation point due to the main flow and this accumulation becomes stronger with decreasing τ up to about $\tau^{-1}=10$. We should note here that the threshold of simple collision model with one-dimensional stagnation flow is $\tau^{-1}=16$.[6] Therefore, qualitative behaviour becomes dif-

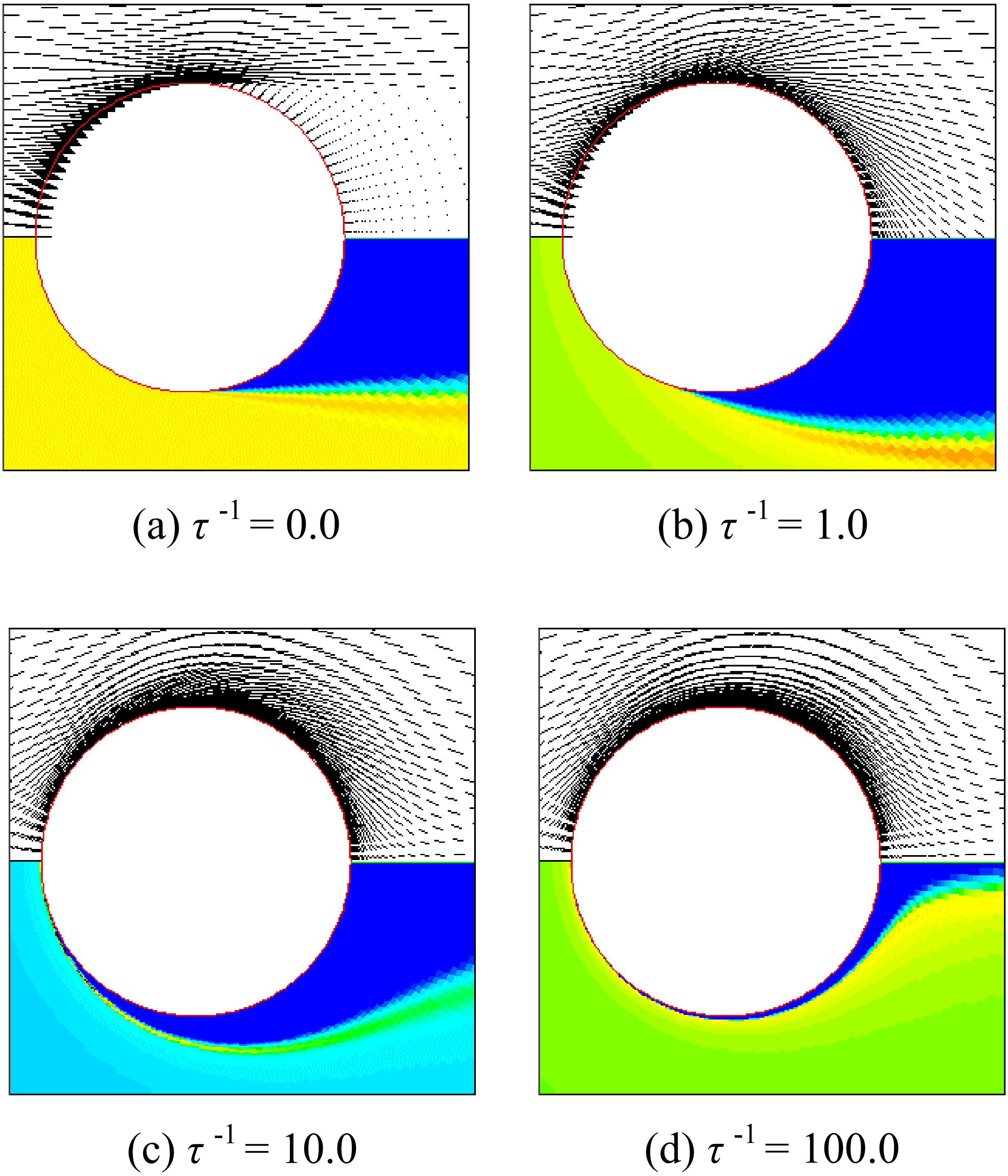

Fig. 2. Velocity and density fields of steady flow of particles around a circular cylinder with potential main flow. Blue colored region in density distribution corresponds to small density of particle.

ferent beyond τ^{-1}~10, in which particle no longer collide with the cylinder. In fact, there exists thin layer of particle free when τ is smaller enough (see (c) and (d)), which was predicted theoretically.[3]

From the profile of particle density and the incoming velocity along the cylinder surface, the local impingement efficiency (β) is obtained as follows,

$$\beta \equiv \eta v \ . \tag{8}$$

We actually consider two kinds of definition of the local impingement efficiency, one of which is defined based on the normal component of the incoming velocity (β_n) and the other is based on the whole length of the velocity vector (β). These two kinds of definition, in particular, play the important role in simulation of accreted ice on a body, respectively.[5],[13] The computational study shows that the distribution of β_n has one peak at the front stagnation point while that of β has two peaks on the both sides of the stagnation.[10]

The total collision efficiency Q is summarized in Fig. 3, which is defined as

$$Q \equiv \oint \beta \, dS \ , \tag{9}$$

where the integral is taken over the cylinder surface.

There are two definitions of Q_n and Q according to the local impingement efficiency β_n and β. The curves decrease drastically in the range of 0.1 to 10. This tendency seems to be the same as the results of main flow based on Navier-Stokes equations.[9]

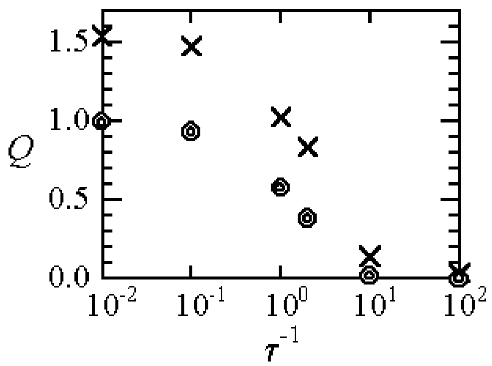

Fig. 3. Total collision efficiency of a stationary cylinder. (◎: Q_n , ×: Q)

3.2 Time-averaged flow fields of oscillating cylinder

Some results of a circular cylinder in pitching and/or heaving oscillation are presented here. In the case of pitching motion, the cylinder rotates periodically around the center while the cylinder moves periodically in translation perpendicular to uniform flow direction in heaving oscillation. Flow fields of particles to four different values of the induced frequency k_p and k_h are depicted in Fig. 4 and 5, respectively. Velocity and density field of particles are shown in upper and lower half of each figure, which are averaged over 10 to 20 periods of the oscillation. It is emphasized that the averaged flow field in Fig. 4 and 5 is not exact since the averaging is not taken at the fixed points in space but moving points. The results, however, seem to be useful to understand the flow fields. In all computations the value of τ keeps the same (=0.5). The value of γ_p is set to 0.1, which means the maximum pitching angle of oscillation is approximately 10 degrees. On the other hand, we use γ_h=0.5 in heaving oscillation.

When k_p is equal to 0.01, the averaged particle flow field seems to be the same as that of a stationary cylinder and the effect of pitching oscillation does not appears. Increasing the value of k_p, the wake region of particles becomes smaller, which can be explained by roll-up/down entrainment behind the cylinder due to the pitching movement. Flow field at k_p=5.0 is somehow different from those in k_p<1.0, in which we can observe some kind of thin layer near the cylinder surface in velocity distribution and large gradient in density field (you actually find black colored area in density distribution of Fig. 4 (d)). In fact, our computation at k_p=10 suffers divergence and the reason has not been clear yet.

When k_h is equal to 0.1, the effect of heaving oscillation does not appear and the particle flow field is the same as that of a stationary cylinder. In the case of pitching motion, downward length of the wake becomes shorter because of flow rolling up into this region. On the other hand, the effect of heaving motion does not appear so clearly at k_h =0.1. The difference is expected from the difference between main potential flows. Instantaneous streamlines of particle flow around a heaving cylinder are obtained by translating those around a stationary cylinder. The effect of heaving motion, therefore, vanishes as long as the oscillation is slow enough comparing with the relaxation time of particle flow. In the case of pitching motion, streamlines are essentially different from those of a stationary cylinder due to the effect of circulation.

We can find the effect obviously at k_h =1.0, in which the wake becomes shorter and the width does larger due to the translation of the cylinder. At k_h =10.0, the wake region spreads over in upstream direction and small density region reaches at the frontal side of the cylinder. In particular, velocity induced by the oscillation becomes dominant than velocity of uniform flow in this case. Averaged velocity near the cylinder surface, therefore, does not vanish because of asymmetry in absorbing boundary condition.

3.3 Total collision efficiency of oscillating cylinder

The feature on the local impingement efficiency and total collision efficiency of oscillating cylinder is summarized as follows.[10]

In the case of pitching cylinder, the profile of local impingement efficiency keeps almost the same as that of a stationary cylinder when k_p<0.1 and we can conclude that the effect of the induced frequency does not appear in k_p<0.1. In this region, the value of β near the position of 45 degrees decreases and the profile becomes wider in the both sides. When a cylinder rotates slowly, the motion of rotation does not affect the particle path. The effect of rotation, therefore, appears as the increment of area on which particle impacts.

The feature of the profile does not change basically in the case of k_p=1.0, in which the width of the profile becomes larger and the value near the stagnation also increases.

On the other hand, the profile in the case of k_p=5.0 is quite different. The width of the profile is the same as that of a stationary case and the value near the position of 45 degrees becomes sharp. This sharpness of the profile seems to come from large gradient of density distribution in the upstream side.

The total amount of collision efficiency Q and Q_n in the pitching oscillation, calculated from the profile of β and β_n according to eq. (9) are shown in Fig. 6. The horizontal broken line means the value of Q in the stationary cylinder. From this result, we can find that the total collision efficiency decreases in pitching oscillation when the oscillation is slow and that the both Q and Q_n increase gradually with increasing k_p.

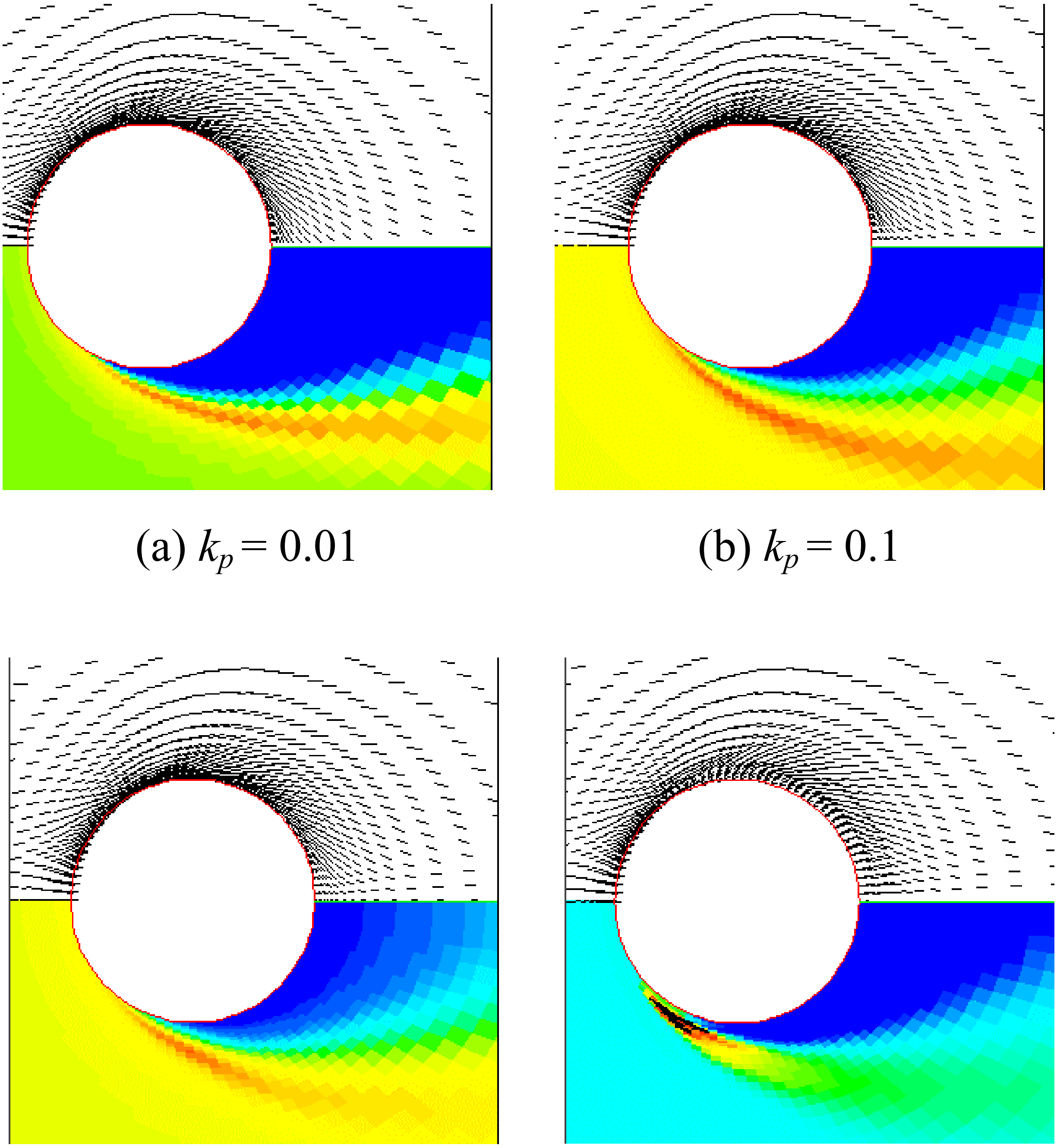

(a) $k_p = 0.01$ (b) $k_p = 0.1$ (c) $k_p = 1.0$ (d) $k_p = 5.0$

Fig. 4. Averaged velocity and density fields of particle flow around a circular cylinder in pitching oscillation. Blue colored region in density distribution also corresponds to small density of particle.

In the case of heaving oscillation, the profile seems to be almost the same as that of a stationary cylinder when k_h<0.01. At k_h=0.1, the value of β near the position of 45 degrees decreases and the profile becomes wider in the both sides. In this case, also, the motion of translation does not affect the particle path when a cylinder translates slowly and the effect of heaving motion appears as the increment of area on which particle impacts as shown in the result of pitching motion (see Fig. 5 (a)).

The feature of the profile becomes rather wider in the case of k_h=1.0, in which the profile spreads over about ±100 degrees portion and the peaks at ±45 degrees of a stationary cylinder vanish completely.

In the case of k_h=10.0, the effect of oscillation becomes dominant comparing with particle flow induced by main flow and the profile spreads further. Actually the non-zero profile reaches at the stagnation point of the downwind side and the total collision efficiency which

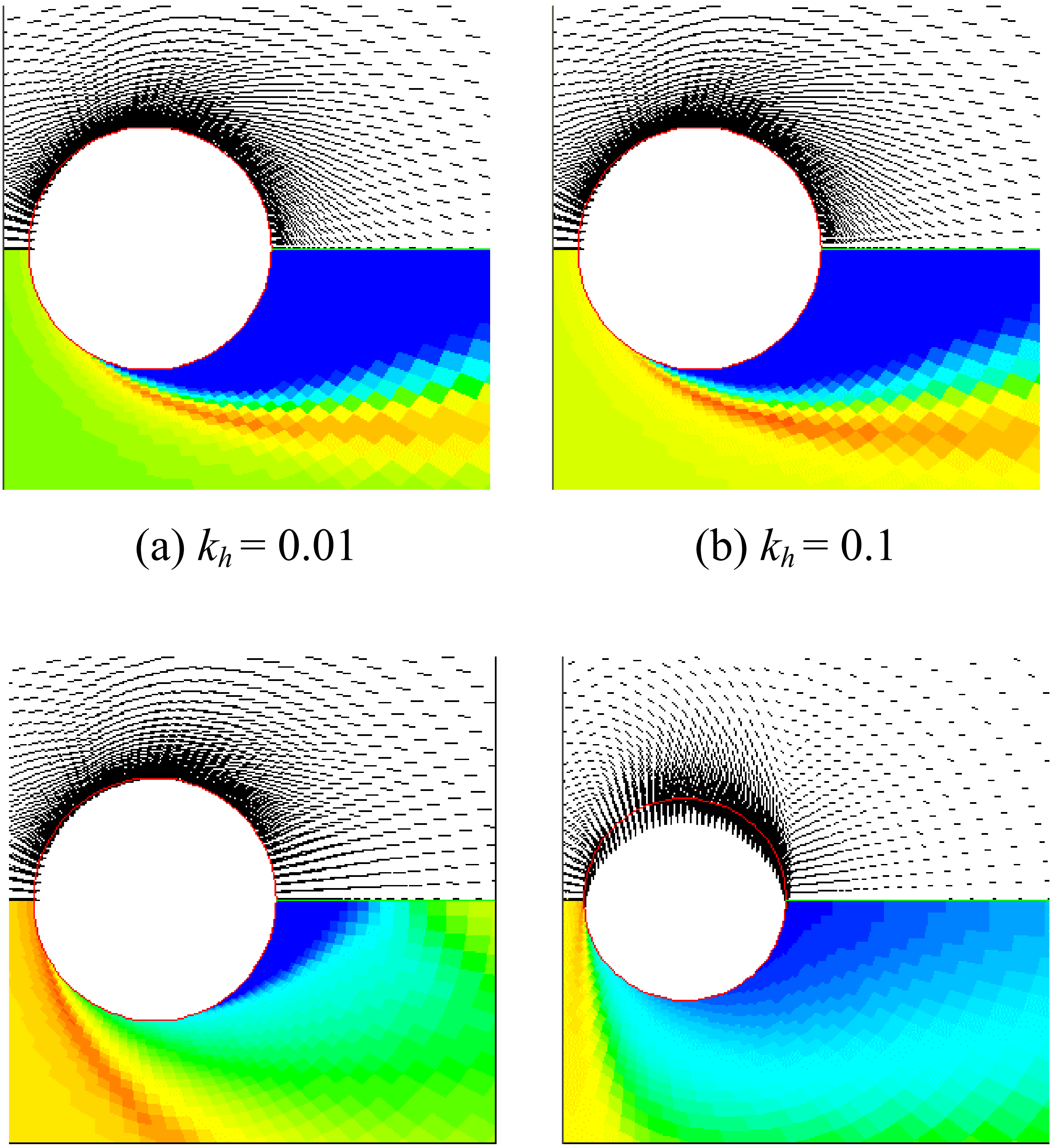

(a) $k_h = 0.01$ (b) $k_h = 0.1$

(c) $k_h = 1.0$ (d) $k_h = 10.0$

Fig. 5. Averaged velocity and density fields of particle flow around a circular cylinder in heaving oscillation. Blue colored region in density distribution also corresponds to small density of particle.

corresponds to the area below the profile, increases obviously.

The total collision efficiency Q and Q_n in the heaving oscillation are shown in Fig. 7. The quantity Q_n increases monotonously with the induced frequency while Q seems to have minimum value at about k_h=1.0. When the induced frequency is large, the motion of oscillation becomes dominant rather than particle flow induced by main flow.

In the case of heaving oscillation, the cylinder in translation moves crossing over streamlines of particles. On the contrary, the pitching motion of the cylinder is almost parallel to streamlines of particle flow and the intercept to particle flow does not occur. This is the reason why the particle amount impacting the cylinder surface increases in the case of heaving oscillation.

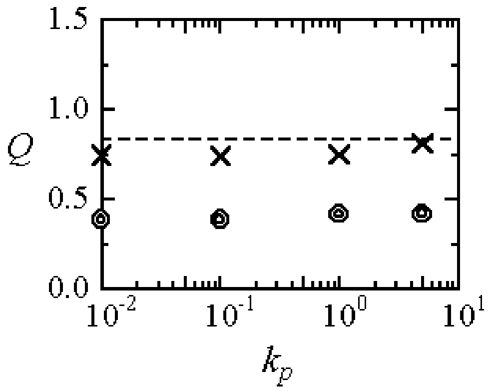

Fig. 6. Total collision efficiency in pitching cylinder. (◎: Q_n , ×: Q)

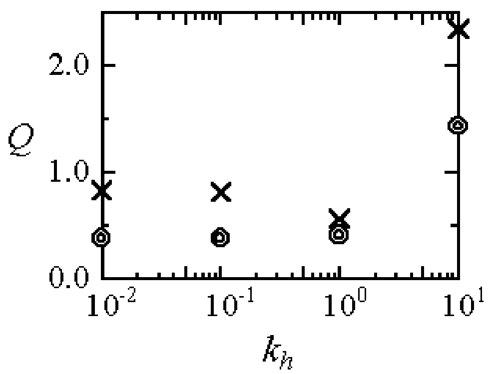

Fig. 7. Total collision efficiency in heaving cylinder. (◎: Q_n , ×: Q)

4. CONCLUSION

Based on two-fluids model of multiphase flow, numerical simulation of particle flow around a circular cylinder is performed in order to clarify the effect of oscillation of a body to particle collision on it. For the simplicity, main flow is assumed to be incompressible potential flow around a circular cylinder with circulation in arbitrary motion.

Computations of a stationary circular cylinder reproduce the behaviour of particle flow field successfully over wide range of the Stokes number τ (non-dimensional relaxation time). In particular, the formation of particle free wake behind the cylinder in infinite τ and that of thin layer of particle free on the cylinder surface in small τ are confirmed, the existence of which is known theoretically.

In particular, the experimental observation on accreted ice shown in Fig. 1 could be explained qualitatively from the present results of an oscillating cylinder in τ=0.5. The shape of accreted ice in heaving oscillation (Fig. 1(c)) is almost the same as that of the stationary case (Fig. 1(a)). On the other hand, in the pitching motion, the growth of accreted ice is found on the both upper and lower sides of the primary ice (Fig. 1(b)).

This work has been supported partly by the Grant-in-Aid for Scientific Research (C) of The Ministry of Education, Science, Sports and Culture.

REFERENCES

(1) Marble, F., E., "Dynamics of dusty gases", Ann. Rev. Fluid Mech., vol. 2, 397-446 (1970).
(2) Saffman, P., G., "On the stability of laminar flow of a dusty gas", J. Fluid Mech., Vol. 13, (1962).
(3) Michael, D. H., "The steady motion of a sphere in a dusty gas", J. Fluid Mech., Vol. 31, part 1, (1968).
(4) Sone, Y., "Flow of dusty gas past a body", J. Phys. Soc. Japan, Vol. 33, No. 1, (1972).
(5) Tsuboi K. and Kimura S., "Numerical Simulation of Ice Accretion on a Body with Droplet Flow Model", AIAA paper 99-3333, (1999).
(6) Langmuir, I. and Blodgett, K., B., "Mathematical Investigation of Water Droplet Trajectories", G. E. Res. Lab. Rep., No. RL 225, (1946).
(7) Kimura, S. and Tsuboi, K., "Wind Tunnel Test for Ice Accretion on an Oscillating Body", Proc. the annual meeting of Japan Soc. of Fluid Mech., 149-150, (1999) in Japanese.
(8) Naterer, G. F., Deng, H. and Popplewell, N., "Predicting and Reducing Glaze Ice Accretion on Electric Power Lines with Joule Heating: Theory and Experiments", Trans. CSME, Vol. 23, No. 1A (1999).
(9) Tsuboi, K. and Kimura, S., "Numerical Study of the Effect of Droplet Distribution in Incompressible Droplet Flows", AIAA-98-2561, (1998).
(10) Tsuboi, K. and Kimura, S.: "Computational Study on Local Impingement Efficiency of an Oscillating Circular Cylinder", AIAA-2000-2661 (2000)
(11) Kawamura, T., Takami, H. and Kuwahara, K., "Computation of high Reynolds number flow around a circular cylinder with surface roughness", Fluid Dynamic Res., Vol. 1, No. 2, (1986).
(12) Tsuboi, K., Tamura, T. and Kuwahara, K., "Numerical Study for Vortex Induced Vibration of a Circular Cylinder in High-Reynolds-Number Flow", AIAA-89-0294, (1989).
(13) Scott, J. N., Hankey, W. L., Giessler, F. J. and Gielda, T. P., "Navier-Stokes Solution to the Flowfield Over Ice Accretion Shapes", J. Aircraft, Vol. 25, No. 8, (1988).